

Analyticity of critical exponents of the $O(N)$ models from nonperturbative renormalization

Andrzej Chlebicki and Paweł Jakubczyk

Institute of Theoretical Physics, Faculty of Physics, University of Warsaw, Pasteura 5, 02-093 Warsaw, Poland

(Dated: May 28, 2022)

We employ the functional renormalization group framework at second order in the derivative expansion to study the $O(N)$ models continuously varying the number of field components N and the spatial dimensionality d . Of our special interest are phenomena occurring in the vicinity of $d = 2$. We in particular address the Cardy-Hamber prediction concerning nonanalytical behavior of the critical exponents ν and η across a line in the (d, N) plane, which passes through the point $(2, 2)$. By direct numerical evaluation of $\eta(d, N)$ and $\nu^{-1}(d, N)$ we find no evidence of discontinuous or singular first and second derivatives of these functions for $d > 2$. The computed derivatives of $\eta(d, N)$ and $\nu^{-1}(d, N)$ become increasingly large for $d \rightarrow 2$ and $N \rightarrow 2$ and it is only in this limit that $\eta(d, N)$ and $\nu^{-1}(d, N)$ as obtained by us are evidently nonanalytical. The derivatives of the exponents show, nonetheless, a locus of maxima located along a line in the (d, N) -plane, with magnitude controlled by the distance from the point $(d, N) = (2, 2)$. This locus is situated close to the expected position of the Cardy-Hamber nonanalyticity line. We provide a discussion of the evolution of the obtained picture upon varying d and N between $(d, N) = (2, 2)$ and other, earlier studied cases, such as $d \rightarrow 3$ or $N \rightarrow \infty$.

I. INTRODUCTION

The $O(N)$ models count among the most paradigmatic systems in the theory of critical phenomena and were with great success applied to address universal characteristics of an amazingly broad variety of physical situations.^{1,2} Even though the physically most relevant cases correspond to integer number of order-parameter components N and integer spatial dimensionality d , it has proven extremely fruitful to consider these quantities formally as continuous parameters, leading to the development of theoretical approaches such as the $(4 - \epsilon)$ -expansion, $(2 + \epsilon)$ -expansion, or the $1/N$ -expansion, where one accesses the most relevant range of parameters ($d = 3$ in particular) by expanding around an analytically soluble point in the (d, N) -plane. It is also worthwhile noting that there has recently been certain interest (both experimental and theoretical) in engineering situations, where the effective dimensionality of the system would not coincide with the physical dimensionality and, in particular, might take a fractional value (see e.g. Refs. 3–5).

A very peculiar physical situation corresponds to $(d, N) = (2, 2)$, representing the Kosterlitz-Thouless (KT) universality class.^{6,7} The vicinity of this point in the (d, N) plane is schematically illustrated in Fig. 1. By infinitesimal variations of (d, N) from the KT point one changes drastically the system behavior, and the anticipated character of this change heavily depends on the direction. The KT universality class is itself very special due to its unique, vortex unbinding driven mechanism of the phase transition. The behavior of the correlation length is controlled by an essential singularity rather than a power law, making it distinct from the transition at any $d > 2$. It follows that the critical exponent $\nu(d, N = 2)$ diverges for $d \rightarrow 2^+$.

The KT case $(d, N) = (2, 2)$ is analytically tractable and it is natural to adopt the $d = 2 + \epsilon$ expansion in an attempt to access also higher dimensionalities. It was this approach that was pursued⁸ by Cardy and Hamber and led to the prediction of the existence of a line [hereafter referred to as Cardy-Hamber (C-H) line] in the (d, N) plane across which the critical exponents would not be analytical functions of (d, N) . The procedure

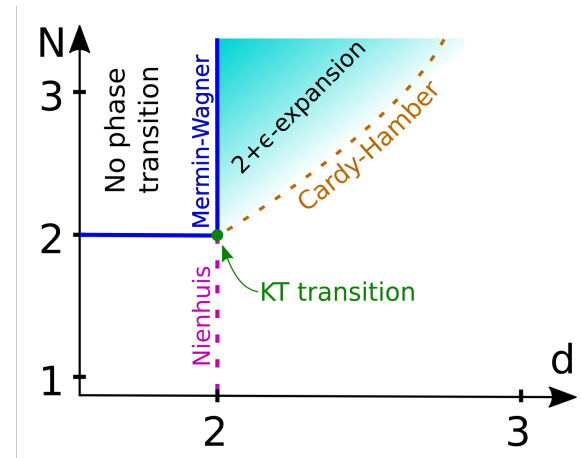


FIG. 1: (Color online) The (d, N) plane in the vicinity of the Kosterlitz-Thouless (KT) point $(2, 2)$, schematically illustrating the landscape of universality classes with some of its most characteristic features. The Mermin-Wagner line separates the regions with possible and impossible symmetry-breaking phase transitions for $N > 2$. The critical exponents are expected to be non-analytical across the Cardy-Hamber line. Exact expressions for the ν^{-1} and η exponents are available along the Nienhuis line [$d = 2$, $N \in (-2, 2)$] as well as in the limit $N \rightarrow \infty$ for $d > 2$.

adopted in Ref. 8 combines the equations studied before by Nelson and Fisher⁹ (valid for $N = 2$, $d \geq 2$ and constituting an extension of the KT equations) with those analyzed by Brézin and Zinn-Justin¹⁰ (valid exclusively for zero vortex fugacity y^2). Under the assumption of analyticity, one may merge the renormalization group (RG) equations from both these studies and interpolate between the two limiting cases. In Ref. 8, this reasoning led to a set of equations for y^2 and the interaction coupling g expanded to the order $O(d - 2, N - 2, y^2)$. The predicted nonanalyticity of the critical exponents arises due to the existence of two distinct solutions to the fixed-point equations. Each of the solutions is physical and describes a criti-

cal point only in a restricted region of the (d, N) -plane. The boundary between these regions defines the C-H line. At the approximation level of Ref. 8, across the C-H line, the fixed points collide and 'swap roles'; which leads to the nonanalyticity of the critical exponents. One consequence⁸ of the supposed nonanalyticity is the restriction of applicability of the $2 + \epsilon$ -expansion to the region above the C-H line (see Fig. 1). As a result of truncating at leading order in $\epsilon = d - 2$, the Cardy-Hamber study does not fully characterize this predicted nonanalyticity. The shape of the C-H line is also evaluated only in a linear approximation around $(d, N) = (2, 2)$; it is nonetheless expected to survive also for higher N , crossing $N = 3$ somewhat below $d = 3$. We note and emphasize that the entire picture is guaranteed to be valid only at this approximation order. It is conceivable that the fixed-point collision is avoided if higher-order terms are taken into account. Our results support this possibility.

In the present paper we revisit the issue of analyticity of the critical exponents from the point of view of nonperturbative RG applied to the ϕ^4 theory. Our motivation follows primarily from the fact that (to the best of our knowledge) the shape of the C-H line seems to have never been calculated beyond the linear order in ϵ . Neither was the character of the expected nonanalyticity of the critical exponents quantified. With this in mind, employing the nonperturbative RG and the derivative expansion (DE) at order ∂^2 , we have scanned the dependence of the critical exponents η and ν^{-1} on (d, N) , with particular focus on the limit $(d, N) \rightarrow (2, 2)$, taken along different paths. Our results indicate no evidently nonanalytical behavior (that would be clearly visible as singularities or discontinuities of any of the first two derivatives) except for $(d, N) = (2, 2)$. The computed derivatives of $\nu^{-1}(d, N)$ and $\eta(d, N)$ exhibit however maxima of magnitude divergent for $(d, N) \rightarrow (2, 2)$ along a line in the (d, N) plane. This locus of maxima turns out to be situated close to the expected position of the C-H line. We computed the profile of this locus in the (d, N) plane both in the vicinity and away from $(d, N) = (2, 2)$.

The paper is structured as follows: In Sec. II we review the (subsequently applied) truncation of functional RG relying on the derivative expansion. In Sec. III we restrict to dimensionality $d = 2$, where the functional forms of the exponents $\nu^{-1}(d = 2, N)$ and $\eta(d = 2, N)$ are exactly known for $N < 2$. We compare our results obtained at order ∂^2 of the DE to the exact values. In Sec. IV we analyze the numerically extracted profiles of $\nu^{-1}(d, N)$ and $\eta(d, N)$ and provide a connection to the C-H prediction. We in particular demonstrate the smoothening of $\nu^{-1}(d, N)$ and $\eta(d, N)$ upon moving away from $(d, N) = (2, 2)$ and emphasize that [after excluding the immediate vicinity of $(d, N) = (2, 2)$] the first two derivatives of these functions show no clear signatures of singular behavior. We identify nonetheless two regimes of the (d, N) plane characterized by distinct (large- N -like and small- N -like) behavior of the critical exponents. Sec. V contains summary and conclusion.

II. FUNCTIONAL RG AND THE DERIVATIVE EXPANSION

We employ the one particle-irreducible variant of nonperturbative RG, adopting the exact Wetterich equation¹¹

$$\partial_k \Gamma_k[\phi] = \frac{1}{2} \text{Tr} \left\{ \partial_k R_k \left[\Gamma_k^{(2)}[\phi] + R_k \right]^{-1} \right\} \quad (1)$$

as the point of departure. Eq. (1) describes the flow of the regularized effective action $\Gamma_k[\phi]$ upon varying the (momentum) cutoff parameter k between the microscopic scale ($k = \Lambda$) and $k \rightarrow 0$. The quantity $\Gamma_k[\phi]$ evolves from the microscopic action $\Gamma_{k=\Lambda}[\phi] = \mathcal{S}[\phi]$ towards the free energy $\Gamma_{k \rightarrow 0}[\phi] = \mathcal{F}[\phi]$ as the infrared cutoff is gradually removed. The latter is implemented by adding a momentum-dependent function R_k to the inverse propagator, which leads to damping of modes with momentum $q < k$ (while leaving the modes with $q > k$ unaffected). The trace in Eq. (1) sums over momentum and components of the order-parameter field ϕ , while $\Gamma_k^{(2)}[\phi]$ denotes the second (functional) field derivative of $\Gamma_k[\phi]$.

The general framework resting upon Eq. (1) was successfully applied in a diversity of contexts over the last years (for reviews see e.g. 12–17). The present study focuses on the canonical case of the $O(N)$ models, where the microscopic action is given by

$$\mathcal{S}[\phi] = \int d^d x \left[\frac{1}{2} (\nabla \phi)^2 + \frac{\lambda}{8} (\phi^2 - \phi_0^2)^2 \right]. \quad (2)$$

Above we restricted to a form valid in the symmetry-broken phase, where the RG flow must be initiated in order to converge for $k \rightarrow 0$ to a fixed point describing the critical state. Note that ϕ is an N -component (real) field. The scheme of derivative expansion proposes an ansatz for the flowing effective action $\Gamma_k[\phi]$, classifying the (symmetry-allowed) terms according to the number of occurring derivatives and truncating terms of order higher than a prescribed value. In the present study we consider the ∂^2 truncation, where $\Gamma_k[\phi]$ is parametrized as

$$\Gamma_k[\phi] = \int d^d x \left\{ U_k(\rho) + \frac{1}{2} (Z_k(\rho) - 2\rho Y_k(\rho)) (\nabla \phi)^2 + \frac{1}{4} Y_k(\rho) (\nabla \rho)^2 \right\}, \quad (3)$$

retaining all the terms involving at most 2 derivatives and truncating those of higher order. Here $\rho = \frac{1}{2} \phi^2$, and the presence of the $Y_k(\rho)$ term distinguishes between the gradient coefficients of the longitudinal and transverse modes. Note that our convention differs from the most standard one (see e.g. Refs. 12, 17, and 18) by subtraction of the term $2\rho Y_k(\rho)$ in the $(\nabla \phi)^2$ coefficient. No truncation of the field dependencies is imposed, so that the set of three flowing functions $\mathcal{F}_k(\rho) = \{U_k(\rho), Z_k(\rho), Y_k(\rho)\}$ is determined by the flow itself and is not constrained by any pre-imposed parameterization. The procedure of projecting the Wetterich equation on the flow of $\mathcal{F}_k(\rho)$ amounts in essence to plugging Eq. (3) into Eq. (1) and is well described in literature (see e.g. Ref. 17).

We note at this point that the longitudinal inverse propagator reads

$$\Gamma_L^{(2)}(q, \rho) = Z_k(\rho)q^2 + U'_k(\rho) + 2\rho U''_k(\rho), \quad (4)$$

while the transverse component of the inverse propagator is evaluated as

$$\Gamma_T^{(2)}(q, \rho) = [Z_k(\rho) - 2\rho Y_k(\rho)]q^2 + U'_k(\rho). \quad (5)$$

The resulting set of three coupled nonlinear partial-differential flow equations can be analyzed numerically. It is convenient to rephrase the flow equations using the dimensionless (rescaled) quantities $\tilde{\rho}$, $u_k(\tilde{\rho})$, $z_k(\tilde{\rho})$, $y_k(\tilde{\rho})$, where

$$\begin{aligned} \rho &= Z_k^{-1} k^{d-2} \tilde{\rho}, \quad U_k(\tilde{\rho}) = k^d u_k(\tilde{\rho}), \quad Z_k(\tilde{\rho}) = Z_k z_k(\tilde{\rho}), \quad (6) \\ Y_k(\tilde{\rho}) &= Z_k^2 k^{2-d} y_k(\tilde{\rho}). \end{aligned}$$

In terms of these, the fixed-point behavior at the critical point is manifest. The rescaling factor Z_k is related to the flowing anomalous dimension via $\eta = -\frac{k}{Z_k} \partial_k Z_k$ and is defined by imposing the condition $z_k(\tilde{\rho}_\eta) = 1$ with $\tilde{\rho}_\eta$ arbitrary. Note that the flowing anomalous dimension is evaluated from the longitudinal component of $\Gamma^{(2)}$. This choice allows for an arbitrary value of N , including $N = 1$, where the transverse modes are absent. We have verified that the differences in our results (relating to the critical point) obtained with η evaluated from the longitudinal or from the transverse directions are negligible. We additionally choose $\tilde{\rho}_\eta = 0$.

Our analysis of the RG equations implements a discretization of the $\tilde{\rho}$ grid and follows two complementary paths. On one hand we integrate the flow starting from the initial condition of Eq. (2) and tune the initial condition so that the flow converges to the fixed point for vanishing cutoff scale. On the other, we solve directly the fixed-point equations. The subsequent linearization around the obtained solution and diagonalization of the obtained matrix allows for identifying the ν^{-1} exponent as the leading (and only positive) eigenvalue. Both methods lead to very similar results, the latter being significantly faster and, in our assessment, also more accurate.

Even though the framework of the derivative expansion was applied over many years, two impressive advancements related directly to the pure $O(N)$ models took place only very recently. The first concerns the resolution of the multicritical fixed point structure, including identification of nonperturbative fixed points in $d = 3$ that had never been found before.¹⁹ The second relates to establishing the methodology of the DE as a high-precision computational approach, capable of providing in $d = 3$ estimates of the critical exponents with accuracy comparable to (or even better than) those delivered by Monte-Carlo simulations and perturbative approaches. This required²⁰ calculations at order ∂^4 of the DE. For the less complex case of Ising symmetry-breaking ($N = 1$) the computation was performed¹⁸ even up to order ∂^6 . In addition to numbers (including errorbars), these studies delivered insights pointing towards rapid convergence of the DE, emphasizing (and clarifying²¹) the role of the so-called principle of minimal sensitivity (PMS).²² The latter amounts to demanding that the analyzed quantity (e.g. a critical exponent) be

(locally) stationary with respect to the regulator choice. The present study utilizes the DE at order ∂^2 , which, however, is entirely sufficient for the purposes described above. We point out that the exactly controlled limits of ($d > 2, N \rightarrow \infty$) as well as ($d = 2, N \leq 2$) are recovered. We note that a somewhat similar scan of the critical indices in the (d, N) plane was performed in Ref. 23 using a simpler truncation of functional RG, where the field dependencies of Z and Y were dropped. For an analogous calculation restricted to $N = 1$ see Ref. 24. The limit $d \rightarrow 2^+$ with $N > 1$ was also examined in Ref. 25 within another simplified functional RG truncation.

A. Regulator choice

In the numerical evaluation of the flow equations we implement the Wetterich cutoff¹²

$$R_k(q) = \alpha Z_k q^2 / [\exp(q^2/k^2) - 1] \quad (7)$$

with a variable parameter α . Refs. 20 and 21 reveal the increasing role of the PMS principle in high-precision evaluation of the critical indices upon elevating the truncation order. At the ∂^2 order of the DE this dependence is however relatively modest. In Fig. 2 we demonstrate the evolution of the PMS value of α varying dimensionality. We find a notable increase of variation of α_{PMS} approaching $d = 2$ and no PMS value in the immediate vicinity of $d = 2$. In $d = 3$ our results for η and ν [e. g. $\eta_{PMS}(d = 3, N = 2) \approx 0.047$ and $\nu_{PMS}(d = 3, N = 2) \approx 0.67$] are close to, (but not fully coincide) with those of Ref. 20 obtained at the ∂^2 truncation order. We attribute this small difference to dropping the terms of order higher than 4 [arising from multiplying the functions $\Gamma^{(3)}$] in the calculation of Ref. 20. In addition, Ref. 20 used a few different families of cutoff functions in providing the final numerical estimates.

In Fig. 3 the PMS value of the exponent η is compared to the value of η obtained for $\alpha = 2$ as function of d . Except for the immediate vicinity of $d = 2$ the difference between the two cases is negligible. The subsequent illustration (Fig. 4) exhibits the dependence of η on α for a sequence of dimensionalities very close to 2.

An alternative procedure of optimizing the regulator was introduced in Ref. 26 specifically for $(d, N) = (2, 2)$. For this case, when integrating the flow in the algebraic (low- T) phase one does not recover the expected line of fixed points exactly, but only in the form of slightly tilted plateaus (quasi-fixed points). The plateau slope can be positive or negative depending on α . One may therefore tune α so that the quasi-fixed point becomes transformed into a true fixed point. This constitutes a phenomenological procedure of compensating the deficiency of the truncation with a 'smart' regulator choice, which however enforces by hand the existence of the fixed-point line in the low- T phase. For T high enough (above the KT phase transition) the fixed point cannot be obtained for any value of α , which signals the normal phase. Ref. 26 identified the 'optimal' value $\alpha_{opt} \approx 2.0$ at $T = T_{KT}$ and $\alpha_{opt}(T) < 2.0$ for $T < T_{KT}$. Note however, that this 'optimal' value (alike PMS) does depend on the renormalization point $\tilde{\rho}_\eta$.

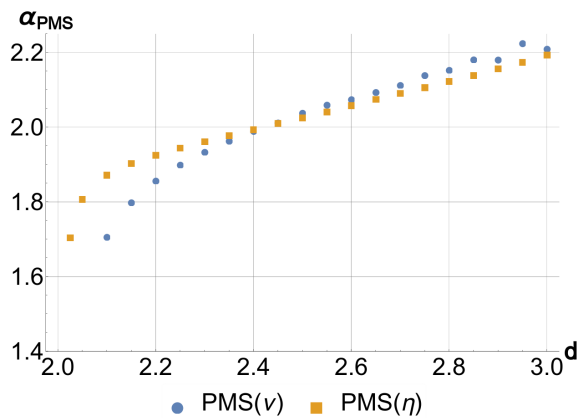


FIG. 2: (Color online) Evolution of the PMS values of the regulator parameter α depending on dimensionality d for $N = 2$. A substantial increase of its variation occurs for d approaching 2. No PMS value is found for d in the immediate vicinity of 2.

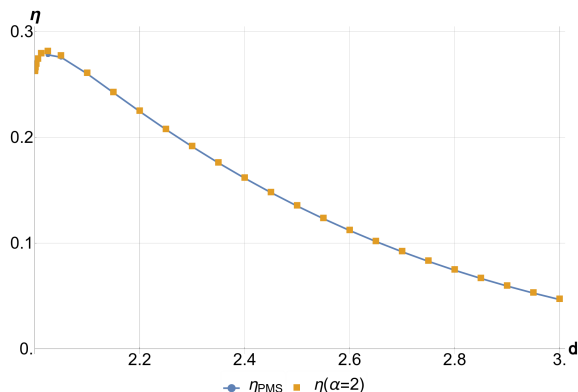


FIG. 3: (Color online) Comparison of exponent η calculated for α_{PMS} and $\alpha = 2$ depending on dimensionality d for $N = 2$.

In what follows we present our results for $\eta(d, N)$ and $\nu^{-1}(d, N)$ as obtained keeping the regulator fixed, with $\alpha = 2.0$. On one hand, this corresponds to an 'average' value for $d \in (2, 3]$ (at least for $N = 2$), on the other it is close to the 'optimal' value for $(d, N) = (2, 2)$. We emphasize that the differences between the PMS values of critical exponents (whenever α_{PMS} can be identified) and the values obtained at $\alpha = 2$ are relatively small. We also verified that the key results of the paper (see Sec.V) are not changed if the PMS regulators are used (whenever they exist, i.e. for d sufficiently separated from 2).

III. DIMENSIONALITY $d = 2$

In this section we analyze the case $d = 2$, approaching $N = 2$ from below. For the KT transition $[(d, N) = (2, 2)]$, the (complete) DE at order ∂^2 was addressed in Refs. 26–28. The

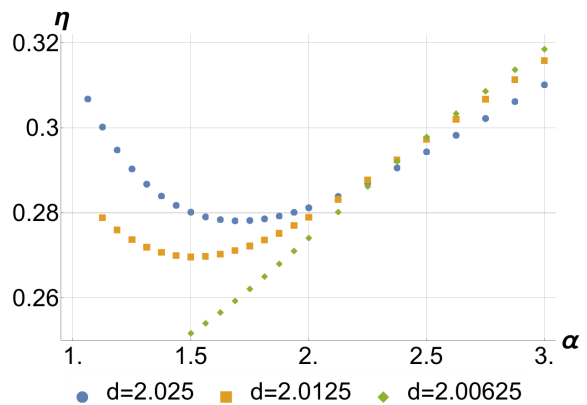


FIG. 4: (Color online) Variation of η depending on α for a sequence of dimensionalities in close vicinity of 2. No PMS value is found for d sufficiently low.

flow equations solved in the present paper are equivalent to those analyzed therein at the fixed point. For studies of the KT transition with other truncations of the functional RG, see Refs. 29–36. We point out that the present approach, despite the lack of vortices present as explicit degrees of freedom, accurately reproduces the key features of the KT transition, including the phase stiffness jump and the essential singularity of the correlation length.

The values of the critical exponents ν^{-1} and η are however exactly known also for $(d = 2, N < 2)$,³⁷ providing a suitable opportunity for further benchmarking our results.

For t defined by $N = -2 \cos(2\pi/t)$, $t \in [1, 2]$ the exact critical exponents read³⁷

$$\nu^{-1} = 4 - 2t, \quad \eta = 2 - t/2 - 3/(2t), \quad (8)$$

and, for $N = 2 - \delta$, can be expanded in δ as follows:

$$\nu^{-1} = \frac{4}{\pi} \sqrt{\delta} + O(\delta), \quad \eta = \frac{1}{4} + \frac{1}{4\pi} \sqrt{\delta} + O(\delta), \quad (9)$$

The first derivatives of both the exponents with respect to N diverge as $N \rightarrow 2^-$, providing a clear indication of nonanalyticity of $\nu^{-1}(d, N)$ and $\eta(d, N)$ at $(d, N) = (2, 2)$.

Fig. 5 presents a comparison between the results obtained by us within the present functional RG truncation and the exact values of the critical exponents. The second-order DE approach yields systematically overestimated values of η and fairly accurate values of ν^{-1} . More importantly, our results capture the nonanalytical behavior of the exponents in the vicinity of $N = 2$. A power-law fit for $\nu^{-1}(d = 2, N)$ in the neighborhood of $N = 2$ yields the exponent 0.45, which is relatively close to the exact value. We note that our results slowly oscillate around the prediction of Nienhuis; we underestimate ν^{-1} very close to $N = 2$, and overestimate it for lower N . As concerns $\eta(d = 2, N)$ in the vicinity of $N = 2$, a power-law fit yields the exponent 0.77, which is clearly overestimated as compared to the exact value $1/2$.

We attribute the inaccuracies concerning the numerical values of the exponents to the low level of the implemented truncation and point out that the case of $d = 2$ is the least favorable

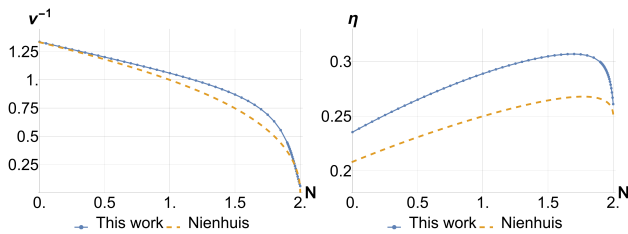


FIG. 5: The critical exponents ν^{-1} and η as functions of N for $d = 2$. The singular first derivatives at $N = 2$ are clearly visible.

for the present approach due to relatively large values of the anomalous dimension.^{17,18,20,21} The accuracy of our method is expected to increase upon raising d . It is nonetheless doubtless from our above results that the second-order DE is able to capture nonanalytic behavior of the critical exponents at $(d, N) = (2, 2)$. In the following section we use an analogous strategy in an attempt to identify the nonanalyticities at $d > 2$ expected to occur along the C-H line.

IV. THE CARDY-HAMBER LINE

In an attempt to detect the C-H line, we identify a (functional) fixed point corresponding to (d, N) located far away from the expected nonanalyticity. This can be done by integrating the flow (tuning the initial condition so that the system flows sufficiently close to a fixed-point solution). We subsequently study the evolution of ν^{-1} and η as either d or N varies towards the region where the C-H line should be found. In practice we either gradually decrease d or increase N . The fixed point at (d, N) serves as the initial condition for the fixed-point equations at $(d - \delta d, N)$ or $(d, N + \delta N)$, which (after discretization) are solved using standard algebraic routines. We are able to scan the (d, N) plane and extract numerically the functions $\eta(d, N)$ and $\nu^{-1}(d, N)$ traversing the region where the C-H line is expected.

In the following subsections we present the results of this scanning procedure along horizontal (subsection A) and vertical (subsection B) trajectories in the (d, N) plane. We note that the procedure of finding the fixed point becomes progressively harder when lowering d and the step in the (d, N) plane must then be tiny. This is (at least partially) related to the fact that the profile of the fixed point effective potential acquires at d low an increasingly strong variation at large $\tilde{\rho}$. For selected choices of (d, N) we checked the results against those obtained by integration of the flow. We note that for $N > 2$ we were not able to solve the fixed-point equations for d arbitrarily close to 2, but anyway significantly lower than the anticipated position of the C-H line.

A. d -dependence

Fig. 6 demonstrates the dependence of the $\nu^{-1}(d)$ exponent on dimensionality for a sequence of values of N . Our results

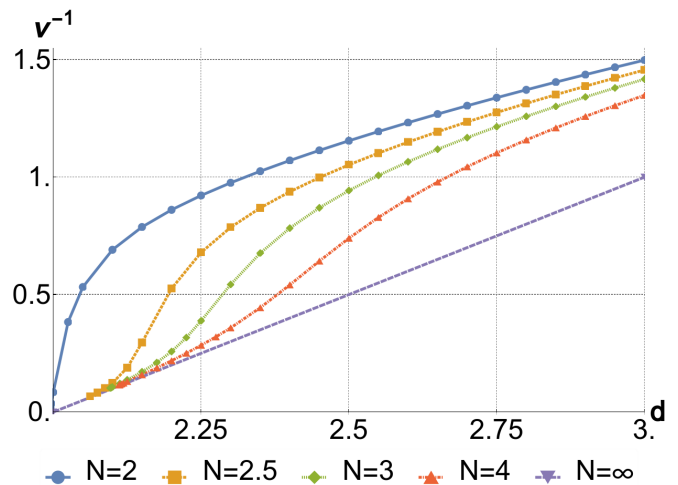


FIG. 6: The exponent ν^{-1} as a function of d for a sequence of values of N .

are juxtaposed with the known exact results $\nu^{-1}(d, N = \infty) = d - 2$. In the limit $d \rightarrow 2^+$, the exponent $\nu^{-1}(d, N = 2)$ vanishes with a very large (presumably infinite) derivative. Only at this point are we dealing with a clear nonanalyticity of ν^{-1} . For each $N > 2$, there exists a characteristic value of dimensionality $d_c(N)$ at which ν^{-1} converges rapidly towards the large- N behavior; $d_c(N)$ increases for growing N .

Our results for the exponent $\eta(d)$ as a function of the dimensionality are presented in Fig. 7 along with the exact result $\eta(d, N = \infty) = 0$. The distinct characteristic of the case $N = 2$ is equally pronounced as for the exponent ν^{-1} . While $\eta(d, N = 2)$ approaches a non-zero value in the limit $d \rightarrow 2$, the curves corresponding to $N > 2$ converge towards 0 in agreement with the ϵ -expansion results.³⁸ As we already remarked, we are not able to get arbitrarily close to $d = 2$ for $N > 2$, however the range of d where the curves in Fig. 7 terminate is significantly lower than the expected position of the C-H line. The dimensionality $d_c(N)$ corresponds to the maximum of $\eta(d)$, where one crosses over between the large- N -like and small- N -like behaviors.

The difference between the behavior of the critical exponents between low- N and large- N regimes fits nicely into the picture presented by Cardy and Hamber and it is natural to relate $d_c(N)$ with the C-H line. We also note that $d_c(N)$ is situated close to the predicted position of the C-H line. However, the crossover from low- N -like to large- N -like behavior remains analytical (or at least of the C^2 type). This suggests that the fixed points' collision described in Ref. 8 is actually avoided within our calculation.

B. N -dependence

The picture becomes even more transparent when we inspect the N -dependence of the critical exponents. Fig. 8 illustrates the variation of ν^{-1} between $N = 1$ and $N = 6$ for a sequence of values of d . These results are compared to the pre-

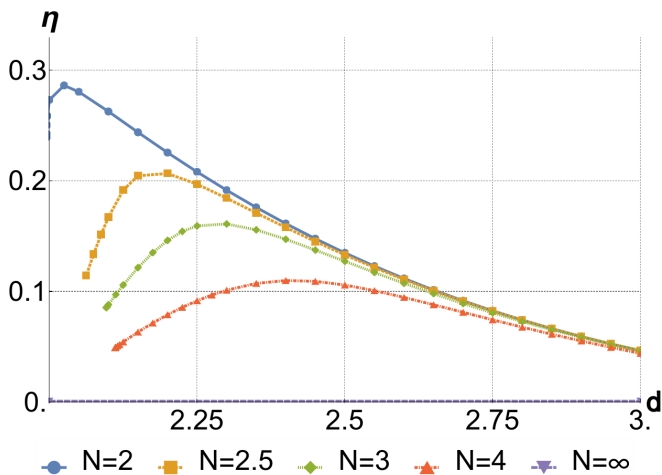


FIG. 7: The exponent η as a function of d for a sequence of values of N .

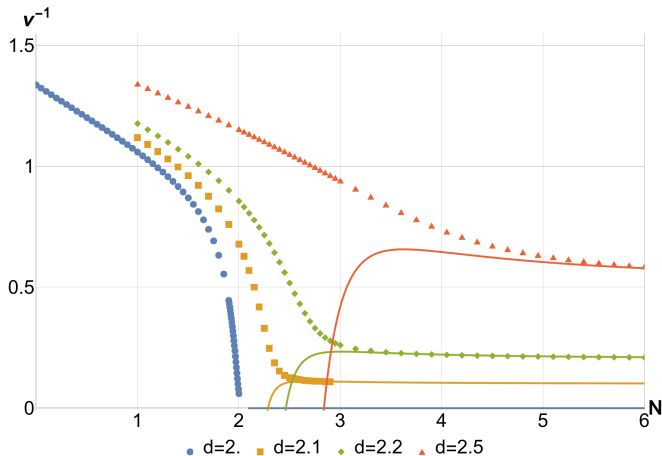


FIG. 8: The exponent ν^{-1} as a function of N for a sequence of values of d . Continuous lines denote the ϵ -expansion predictions.

dictions of the ϵ -expansion at order ϵ^4 .³⁸ In two dimensions, ν^{-1} approaches 0 in a square-root like fashion, exhibiting the nonanalyticity at $N = 2$. At higher dimensions ν^{-1} reaches the large- N limit, but no clear nonanalyticity is present. Instead, a crossover-like behavior between low- N and large- N regimes occurs. This crossover smoothens progressively upon increasing d . This transition seems to be closely related to the point where the divergence between our results and the predictions of the ϵ -expansion occurs.

Fig. 9 displays a comparison between our results for the exponent η and the predictions of the ϵ -expansion. At the point $(d, N) = (2, 2)$, η has a discontinuity and a singular derivative. These two properties do not survive when we move to larger dimensions; $\eta(d > 2, N)$ slowly approaches its large- N limit ($\eta(d, N = \infty) = 0$) in an apparently analytical fashion. Our results indicate that the nonanalyticity of the critical exponents present at $(d, N) = (2, 2)$ becomes smoothed as we move to higher dimensions.

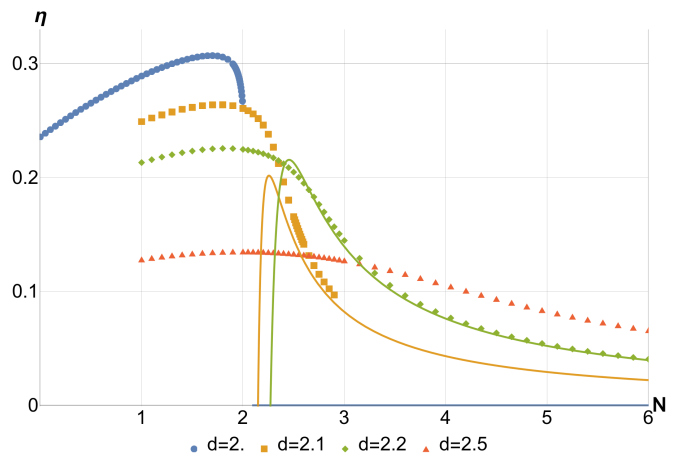


FIG. 9: The exponent η as a function of N for a sequence of values of d . Continuous lines denote the ϵ -expansion predictions.

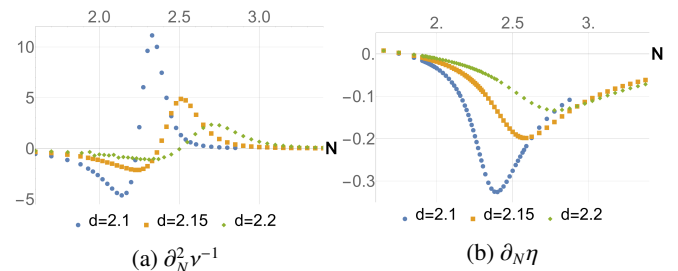


FIG. 10: The derivatives of the critical exponents as functions of N for a sequence of values of d .

We finally examine the derivatives of the critical exponents $\nu^{-1}(d, N)$ and $\eta(d, N)$, which diverge in the limit $(d, N) \rightarrow (2, 2)$. The first derivative of ν^{-1} jumps from $-\infty$ to 0 upon crossing $N = 2$, therefore we analyze the maxima of $\partial_N^2 \nu^{-1}$. For similar reasons, we inspect the minima of $\partial_N \eta$. The values at their extrema are increasingly large as the $\epsilon = d - 2$ approaches 0, yet they become infinite only in this limit. Fig. 10 illustrates the behavior of these relevant derivatives.

The maxima of $\partial_N^2 \nu^{-1}$ and the minima of $\partial_N \eta$ lie very close to each other. The values of the derivatives at maxima become increasingly small as d grows; between $d = 2.75$ and $d = 3$, the maximum of $\partial_N^2 \nu^{-1}$ disappears completely. The loci of the maxima of $\partial_N^2 \nu^{-1}$ and the minima of $\partial_N \eta$ are plotted in Fig. 11 in the (d, N) plane. In the vicinity of $(d, N) = (2, 2)$, they are found very close to the Cardy-Hamber line.

V. CONCLUSION

In this paper we have addressed the analyticity of the critical exponents $\nu(d, N)$ and $\eta(d, N)$ of the $O(N)$ models in $d \geq 2$, $N \geq 2$, varying continuously dimensionality d and the number of order parameter components N . We confronted our results obtained from functional renormalization group (trun-

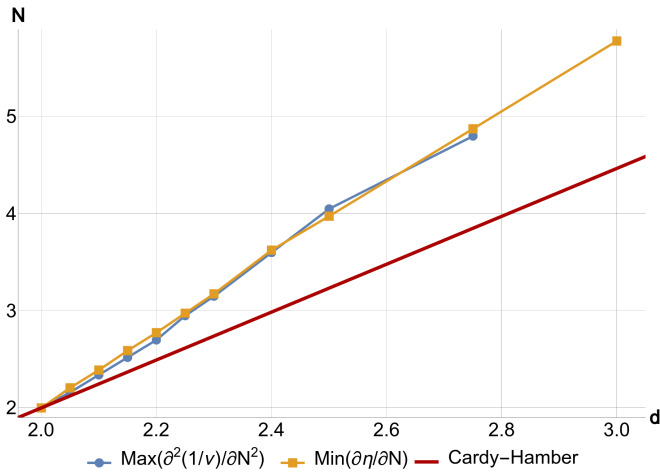


FIG. 11: Loci of the maxima of $\partial_N^2 v^{-1}$ and the minima of $\partial_N \eta$ compared to the C-H line.

cated at order ∂^2 of the derivative expansion) against those derived long ago by Cardy and Hamber within the $2 + \epsilon$ expansion⁸ of the non-linear sigma model at order ϵ . Except for $(d, N) = (2, 2)$ we did not recover signatures of non-analyticities of the critical exponents that would be manifest from the properties of the first two derivatives of the functions $v^{-1}(d, N)$ and $\eta(d, N)$. Instead, we obtained a locus of maxima of the derivatives of the functions $v^{-1}(d, N)$ and $\eta(d, N)$, terminating with a singularity at $(d, N) = (2, 2)$ and a related crossover of the critical exponents between large- N -like and

small- N -like regimes. This constitutes an apparent disagreement with the results of Ref. 8. We are not able to give a complete and final resolution of this puzzle relying on the present calculation. We note however, that the prediction of Cardy-Hamber involves the phenomenon of fixed-point collision, which may well be avoided when terms of higher order in ϵ are taken into account. We also cannot exclude the possibility that the locus of derivatives' maxima obtained by us at the present truncation level (order ∂^2 of the derivative expansion) is in fact a 'fingerprint' of the Cardy-Hamber line, which would build up into a true nonanalyticity upon including higher-order terms of the derivative expansion, indicating that the present framework is insufficient to capture the rather subtle 'fixed point collision' phenomenon. This insufficiency would apply both to the vicinity of $(d, N) = (2, 2)$, as well as larger dimensions, where our approximation scheme is expected to become increasingly more reliable^{18,20} due to the decreasing value of the anomalous dimension η . Finally, it is not excluded that $v(d, N)$ and $\eta(d, N)$ are non-analytical functions belonging to the C^2 class.

ACKNOWLEDGMENTS

We thank Bertrand Delamotte for his help at the initial stages of this project and Nicolas Wschebor for a useful correspondence on related topics. We are grateful to Maxym Dudka for discussions as well as reading the manuscript and providing suggestions on the manuscript. We acknowledge support from the Polish National Science Center via grant 2017/26/E/ST3/00211.

-
- ¹ D. J. Amit, *Field Theory, the Renormalization Group, and Critical Phenomena* (World Scientific, 1984).
 - ² J. Zinn-Justin, *Phase Transitions and Renormalization Group* (Oxford University Press, 2007).
 - ³ O. Boada, A. Celi, J. I. Latorre, and M. Lewenstein, *Phys. Rev. Lett.* **108**, 133001 (2012).
 - ⁴ O. Boada, A. Celi, J. Rodríguez-Laguna, J. I. Latorre, and M. Lewenstein, *New Journal of Physics* **17**, 045007 (2015).
 - ⁵ M. Łebek and P. Jakubczyk, *Phys. Rev. A* **102**, 013324 (2020).
 - ⁶ J. M. Kosterlitz and D. J. Thouless, *Journal of Physics C: Solid State Physics* **6**, 1181 (1973).
 - ⁷ P. M. Chaikin and T. C. Lubensky, *Principles of condensed matter physics* (Cambridge University Press, 1995).
 - ⁸ J. L. Cardy and H. W. Hamber, *Phys. Rev. Lett.* **45**, 499 (1980).
 - ⁹ D. R. Nelson and D. S. Fisher, *Phys. Rev. B* **16**, 4945 (1977).
 - ¹⁰ E. Brézin and J. Zinn-Justin, *Phys. Rev. Lett.* **36**, 691 (1976).
 - ¹¹ C. Wetterich, *Physics Letters B* **301**, 90 (1993).
 - ¹² J. Berges, N. Tetradis, and C. Wetterich, *Physics Reports* **363**, 223 (2002).
 - ¹³ J. M. Pawłowski, *Annals of Physics* **322**, 2831 (2007).
 - ¹⁴ P. Kopietz, L. Bartosch, and F. Schütz, *Introduction to the Functional Renormalization Group* (Springer Verlag, 2010).
 - ¹⁵ J. Polonyi and A. Schwenk, eds., *Renormalization Group and Effective Field Theory Approaches to Many-Body Systems* (Springer Verlag, 2012).
 - ¹⁶ W. Metzner, M. Salmhofer, C. Honerkamp, V. Meden, and K. Schönhammer, *Rev. Mod. Phys.* **84**, 299 (2012).
 - ¹⁷ N. Dupuis, L. Canet, A. Eichhorn, W. Metzner, J. M. Pawłowski, M. Tissier, and N. Wschebor, arXiv:2006.04853 (2020).
 - ¹⁸ I. Balog, H. Chaté, B. Delamotte, M. Marohnić, and N. Wschebor, *Phys. Rev. Lett.* **123**, 240604 (2019).
 - ¹⁹ S. Yabunaka and B. Delamotte, *Phys. Rev. Lett.* **119**, 191602 (2017).
 - ²⁰ G. De Polsi, I. Balog, M. Tissier, and N. Wschebor, *Phys. Rev. E* **101**, 042113 (2020).
 - ²¹ I. Balog, G. De Polsi, M. Tissier, and N. Wschebor, *Phys. Rev. E* **101**, 062146 (2020).
 - ²² L. Canet, B. Delamotte, D. Mouhanna, and J. Vidal, *Phys. Rev. B* **68**, 064421 (2003).
 - ²³ A. Codello, N. Defenu, and G. D'Odorico, *Phys. Rev. D* **91**, 105003 (2015).
 - ²⁴ H. Ballhausen, J. Berges, and C. Wetterich, *Physics Letters B* **582**, 144 (2004).
 - ²⁵ A. Codello and G. D'Odorico, *Phys. Rev. Lett.* **110**, 141601 (2013).
 - ²⁶ P. Jakubczyk, N. Dupuis, and B. Delamotte, *Phys. Rev. E* **90**, 062105 (2014).
 - ²⁷ G. v. Gersdorff and C. Wetterich, *Phys. Rev. B* **64**, 054513 (2001).
 - ²⁸ P. Jakubczyk and A. Eberlein, *Phys. Rev. E* **93**, 062145 (2016).
 - ²⁹ M. Gräter and C. Wetterich, *Phys. Rev. Lett.* **75**, 378 (1995).

- ³⁰ S. Nagy, I. Nándori, J. Polonyi, and K. Sailer, Phys. Rev. Lett. **102**, 241603 (2009).
- ³¹ A. Rançon and N. Dupuis, Phys. Rev. B **89**, 180501 (2014).
- ³² A. Rançon and N. Dupuis, Phys. Rev. B **96**, 214512 (2017).
- ³³ P. Jakubczyk and W. Metzner, Phys. Rev. B **95**, 085113 (2017).
- ³⁴ J. Krieg and P. Kopietz, Phys. Rev. E **96**, 042107 (2017).
- ³⁵ N. Defenu, A. Trombettoni, I. Nándori, and T. Enss, Phys. Rev. B **96**, 174505 (2017).
- ³⁶ I. Maccari, N. Defenu, L. Benfatto, C. Castellani, and T. Enss, Phys. Rev. B **102**, 104505 (2020).
- ³⁷ B. Nienhuis, Phys. Rev. Lett. **49**, 1062 (1982).
- ³⁸ H. Kleinert, Phys. Lett. Sect. A Gen. At. Solid State Phys. **264**, 357 (1998), arXiv:9808145 [hep-th].